Second Conference on Smart Monitoring,
Assessment and Rehabilitation of Civil Structures

SMAR 2013

Stress Concentration and Failure of Perforated CFRP Lamella under Unidirectional Tension

Yue Liu[1], Bernd Zwingmann[2], Mike Schlaich[3] and Ralf Goller[4]

[1,2,3] Technical University of Berlin, Berlin, Germany
[4] SGL Technologies GmbH, Meitingen, Germany

ABSTRACT: Carbon fibre reinforced polymer (CFRP) has many advantages, such as high specific strength, anti-fatigue and anti-corrosion, which make it an excellent alternative to metal materials in aerospace, automotive and construction industry. In order to connect or anchor CFRP components, it is often necessary to insert holes into them. In view of this situation, this paper summarises the investigation of unidirectional CFRP lamellas with a central circular hole under unidirectional tension via theoretical equations, finite element method (FEM) and experiment. Firstly, the stress distribution in fibre direction near the hole is analysed and compared with the case of steel lamellas. A suggested stress concentration factor (*SCF*) for centrally perforated CFRP lamellas with a finite width is proposed. Then, the failure location of CFRP lamellas are determined with the FEM software ABAQUS using strength criterions and verified by an experiment. The failure process is also simulated with FEM using Hashin criterion and verified by observation during the experiment.

1 INTRODUCTION

Carbon fibre reinforced polymer (CFRP) is composed of carbon fibres embedded in polymer matrix. It was firstly used in military industry about 60 years ago. Due to its advantageous properties like high specific strength, corrosion resistance and fatigue resistance, CFRP has now emerged as a practical material for numerous applications in aerospace, automotive and construction industries.

The mechanical properties of carbon fibre are typically orders of magnitude greater than those of polymer matrix. Therefore CFRP shows strong orthotropic characteristics. In the fibre direction, CFRP mainly presents the fibre’s mechanical properties, such as high strength and high Young’s modulus. Perpendicular to the fibre direction, CFRP mainly presents the polymer’s mechanical properties, whose stiffness and resistance is relatively small. Low strength and modulus in transverse direction makes CFRP components hard to be connected or anchored. A summary of possible anchorages for CFRP tension members can be found in (Schlaich et al. 2012). Perforated connections and anchorages, which are very commonly used in metal structures, should be treated with more caution when applied to CFRP. In view of this situation, research was done on the CFRP lamellas with a central circular perforation under unidirectional tension in this paper (Figure 1).

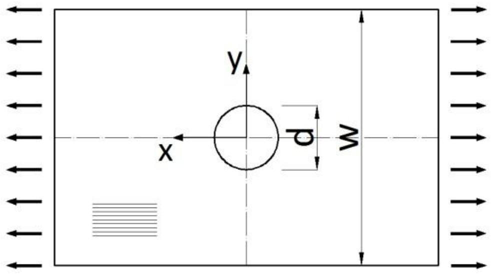

Figure 1. Centrally circularly perforated CFRP lamella with tension in fibre direction.

There are already some existing research achievements about this topic. Tan (1994) established an approximate method for analysing the stress concentration in a circularly or elliptically perforated composite plate. Based on the Lekhnitski Theory (Lekhnitski 1984), Giulio (2001) applied the consolidated variable method to analyse the strain and stress distribution near the hole of an orthotropic plate under uniaxial tension, biaxial tension and shearing stress. Wu and Mu (2003) extended the application of *SCF* of isotropic material to orthotropic material, and found an empirical equation for calculating the *SCF* in an orthotropic plate or shell with a circular opening. These investigations are mainly based on the theoretical derivation and experiment results, but no on fine FEM simulation. In order to fill the gap, in this paper a series of fine FEM models is applied to study the stress distribution and to simulate the failure process of CFRP lamellas. The analysis results were compared with the results from steel lamellas and verified by the experiment.

2 THE STRESS CONCENTRATION NEAR THE HOLE

The stress concentration near the hole is investigated using three different methods, which are the FEM analysis, the experiment and the analytic equation.

2.1 FEM analysis for the case of CFRP lamella with finite width

As a base for this paper, FE models of ten centrally circularly perforated CFRP lamellas with different widths under unidirectional tension are calculated using ABAQUS. The stress concentration in the *x*-direction near the hole is analysed and the distribution of σ_x is obtained. In order to compare, ten geometrically equal models with steel material were created and analysed. The material characteristics of CFRP and steel lamellas used in the FEM calculation are listed in table 1.

Table 1. Material properties used in the analysed FE models

Material	E_x [GPa]	E_y [GPa]	μ_{yx} [-]	μ_{xy} [-]	G_{xy} [GPa]	G_{xz} [GPa]	G_{yz} [GPa]
CFRP lamella	156	9.3	0.27	0.02	4.7	4.7	3.4
Steel	210	210	0.3	0.3	81	81	81

The thickness of the modelled lamellas is 0.7 mm and the diameter of central circular hole is 3.5 mm. The length of the lamella is 180 mm and its width varies from 18 mm to 180 mm. The unidirectional tension load for all models is 200 MPa. Because of geometric symmetry, 1/4 of the lamella was selected to create the model. One typical FE model is shown in Figure 2. The other models are similar to it.

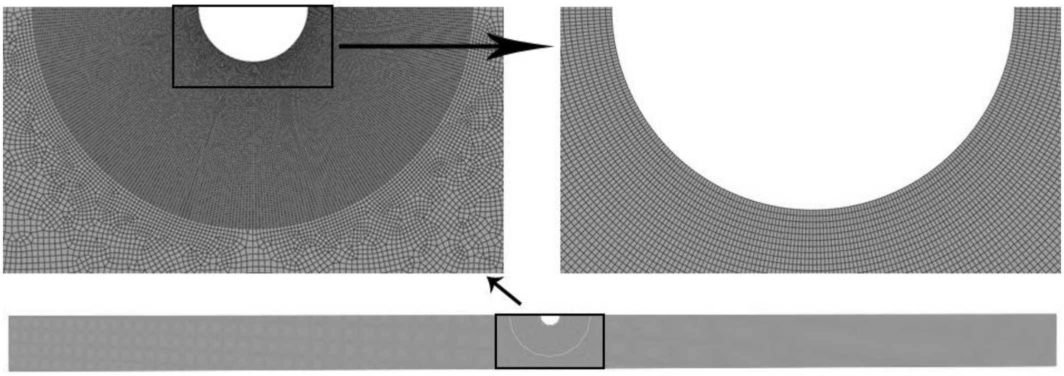

Figure 2. FE model of a CFRP lamella in ABAQUS.

The element type used for the model is a 4-node doubly curved general-purpose plane shell element (S4). The approximate maximum edge length of each element is 0.2 mm. Close to the hole the mesh was refined to 1/5 of the global element size. Going on to refine the mesh, the difference of stress results stays lower than 5% so that the mesh used in the analysis is considered to be fine enough.

The stress concentration of σ_x near the hole of CFRP lamellas is shown in Figure 3 for two geometric configurations.

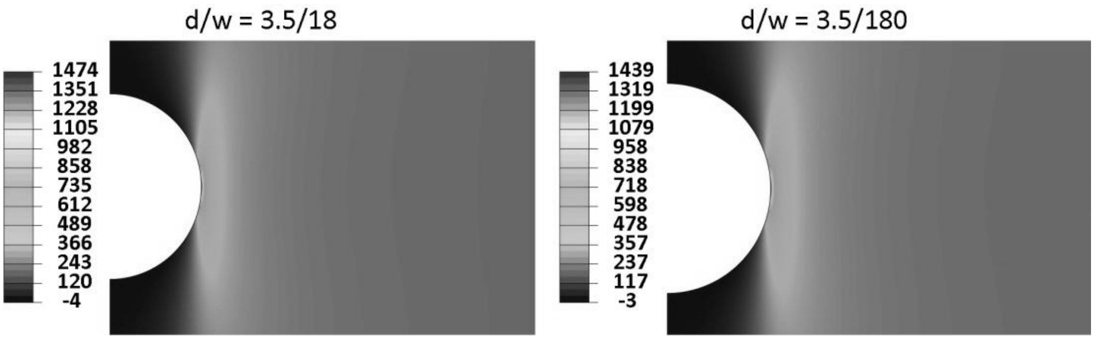

Figure 3. Stress concentration in *x*-direction of CFRP lamellas for different *d*/*w* ratios [MPa].

For comparison, the stress concentration of σ_x close to the hole of two corresponding steel lamellas is shown in Figure 4.

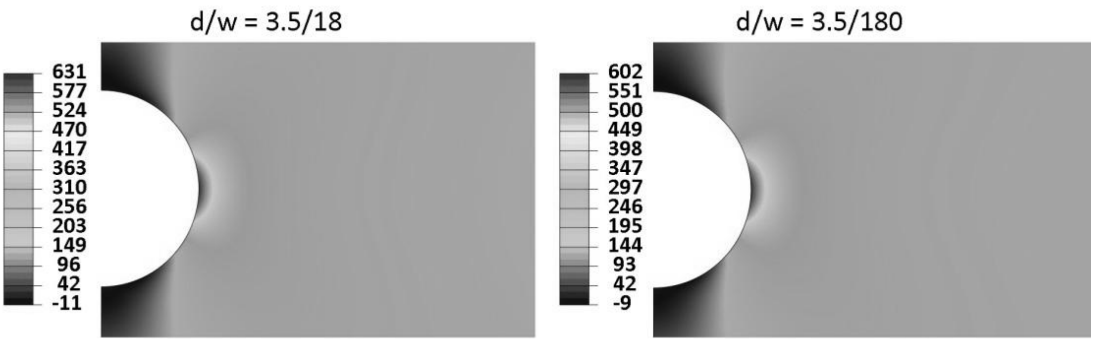

Figure 4. Stress concentration in *x*-direction of steel lamellas for different *d*/*w* ratios [MPa].

The maximum stress value for the all analysed models is summarized in table 4.

Table 4. Maximum value of σ_x for different *d*/*w* ratios [MPa]

d/*w* ratio	3.5 / 18	3.5 / 36	3.5 / 54	3.5 / 72	3.5 / 90	3.5 / 108	3.5 / 126	3.5 / 144	3.5 / 162	3.5 / 180
CFRP	1474	1446	1442	1440	1440	1439	1439	1439	1439	1439
Steel	631	609	605	604	603	603	603	602	602	602

It can be seen from Figure 3 that σ_x is concentrated at the transverse side of the hole. At the longitudinal side of the hole it has a small negative value. When *d*/*w* equals 3.5/18, the maximum stress is 1474 MPa. With the increase of width and the decrease of *d*/*w* ratio, the peak values also decrease. When *d*/*w* reaches 3.5/108 (see table 4), the peak is reduced to 1439 MPa and will not reduce any more by increasing the width.

Table 4 also shows the σ_x concentration in the corresponding steel lamellas. The stress peak for a *d*/*w* ratio of 3.5/18 equals 631 MPa. Like in the case of CFRP lamellas, the stress peak values reduce with the increase of the width. When the *d*/*w* ratio reaches 3.5/144, the peak is 602 MPa and does not reduce any more increasing the width. At this time, the lamella is assumed as approximately infinitely wide and its stress concentration factor is 602 MPa / 200 MPa = 3.01, which is in accordance with the theoretical result (*SCF* = 3.0) for an isotropic circularly perforated lamella with infinite width (Timoshenko & Gere 1961). The consistency proves that the used FEM analysis is correct.

The distribution curves of σ_x from CFRP and steel lamellas along the *y*-axis at one side of the hole are drawn for two *d*/*w* ratios in Figure 5, where y equals the distance from the hole edge to the corresponding point.

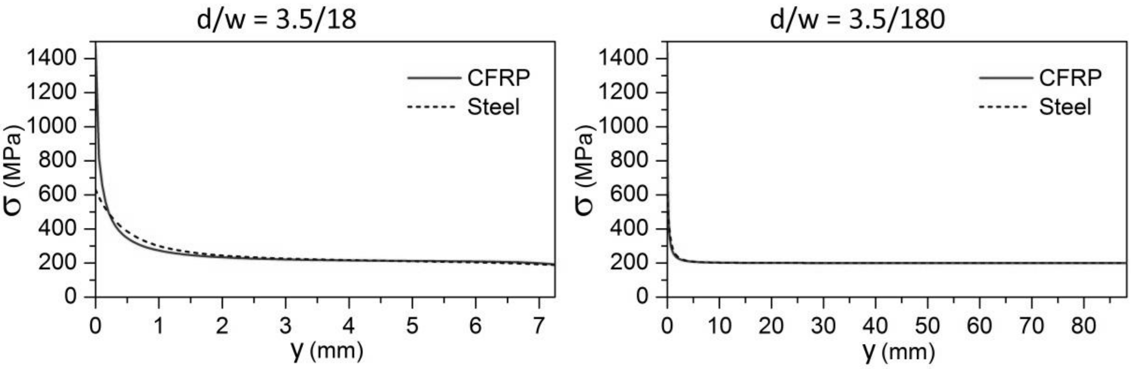

Figure 5. σ_x distribution curves along *y*-axis at one side of the hole.

Comparing Figure 3 and Figure 4, it can be seen that the maximum stress value in CFRP lamellas is much higher than that in corresponding steel lamellas. From Figure 5, one can observe that σ_x declines faster in CFRP lamellas than in steel lamellas, although their shapes are similar. These two phenomena are mainly caused by the strong orthotropic properties of CFRP lamellas.

2.2 *Experiment verification for the FEM results*

In order to verify the FEM results, centrally circularly perforated CFRP lamellas are tested under uniaxial tension to measure the distribution of σ_x and draw the stress distribution curve. The four equal specimens have the dimensions length = 180 mm, width = 18 mm and thickness = 0.7 mm. The diameter of central hole is 3.5 mm (*d*/*w* = 3.5/18). A photo of one CFRP lamella specimen is shown in Figure 6.

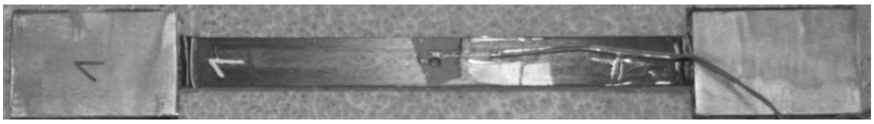

Figure 6. A CFRP lamella specimen with a perforated hole.

All lamellas are tensioned until failure. During the test, the σ_y distribution along the *x*-axis is measured on one side of the hole by strain gauges. Based on the experiment data, the σ_y distribution is drawn for a tension load of 200 MPa. In Figure 7 the obtained curve is compared with the FEM result.

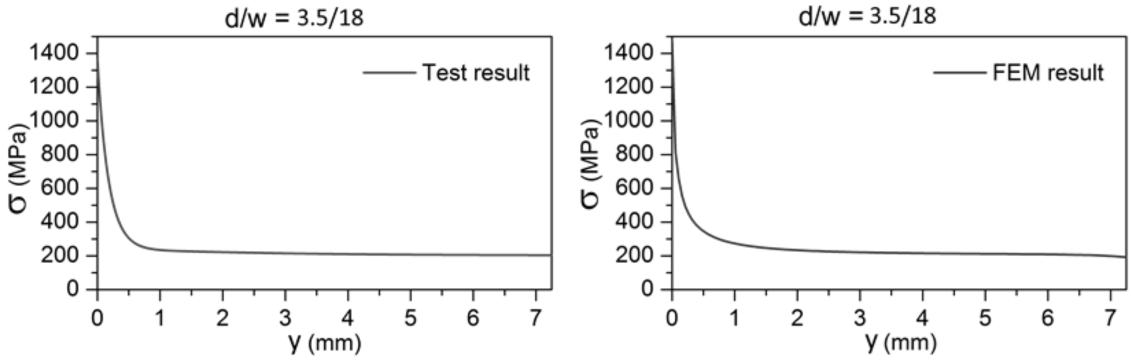

Figure 7. σ_x distribution curve from experiment and FEM analysis.

It can be seen from Figure 6 that the results of the experiment generally agree with those of the FEM analysis. But the stress peak value obtained from the FEM calculation (1474 MPa) is higher than that from the experiment (1362 MPa) with a difference of 7.6%. This is possibly caused by two effects. Firstly, the strain gauge cannot be located exactly at the edge of the hole. Secondly, the plastic behaviour of the resin may reduce the stress peak, which is not considered in the FEM analysis.

2.3 *Experimental semi-empirical equation for calculating the SCF for centrally circularly perforated CFRP lamella with finite width*

On the basis of classical elasticity theory (Gibson 2007), the *SCF* for circularly perforated orthotropic plate with infinite width under unidirectional tension K_i can be written as

$$K_i = 1 + \sqrt{2\left(\sqrt{\frac{E_x}{E_y}} - \mu_{xy}\right) + \frac{E_x}{G_{xy}}}\ . \qquad (1)$$

In which, E_x is elastic modulus in fibre direction, E_y the elastic modulus in perpendicular to the fibre direction, μ_{xy} the Poisson’s ratio and G_{xy} is shear modulus in *x-y* plane.

In the realized investigation the *d*/*w* ratio is more than 3.5/108. Thus the lamella can be considered as infinitely wide and the *SCF* can be calculated as 1439 MPa / 200 MPa = 7.2. Substituting the material properties from table 1 into equation (1), one can gain K_i = 7.43 with a difference of 3.1 % between the FEM result and the theoretical result. K_f for the case of a finite width can be gained by multiplying equation (1) with the geometry dependent coefficient *C(d/w)*.

$$K_f = C(d/w) \cdot \left\{ 1 + \sqrt{2\left(\sqrt{\frac{E_x}{E_y}} - \mu_{xy}\right) + \frac{E_x}{G_{xy}}} \right\} \tag{2}$$

Based on the elastic theory and the FEM results from this paper, *C(d/w)* can be written as:

$$C(d/w) = \left[1 - \frac{1}{2}\left(\frac{d}{w}\right)^2 - \frac{1}{2}\left(\frac{d}{w}\right)^4 + 5(K_i - 3) \cdot \left\{ \left(\frac{d}{w}\right)^6 - \left(\frac{d}{w}\right)^8 \right\} \right]^{-1} \tag{3}$$

The calculation results from equation (2) with different *d*/*w* ratio are compared with the FEM results from section 2.1 and listed in table 4.

Table 4. Comparison of the *SCF* calculated with equation (2) and FEM

d/*w* ratio	3.5 / 18	3.5 / 36	3.5 / 54	3.5 / 72	3.5 / 90	3.5 / 108	3.5 / 126	3.5 / 144	3.5 / 162	3.5 / 180
Equation (2)	7.57	7.47	7.45	7.44	7.44	7.43	7.43	7.43	7.43	7.43
FEM	7.37	7.23	7.21	7.20	7.20	7.20	7.20	7.20	7.20	7.20
Error [%]	2.6	3.2	3.2	3.2	3.2	3.1	3.1	3.1	3.1	3.1

As can be seen from table 4, the results from equation (2) coincide well with the FEM results. It may be used to predesign perforated finite lamellas without using FEM analysis. The applicability should be checked in engineering practice.

3 THE FAILURE OF CFRP LAMELLAS

Because of the strong orthotropic characteristics, the strength of CFRP lamellas in different directions may have great difference. Hence, the failure location of perforated CFRP lamellas is probably different from that of perforated steel lamellas. In steel lamellas the failure starts at the σ_x peak point. For a CFRP lamella the σ_y and τ distribution close to the hole is shown in Figure 8 for a tension load of 200 MPa and a *d*/*w* ratio of 3.5/18, which is the geometry of the tested specimens.

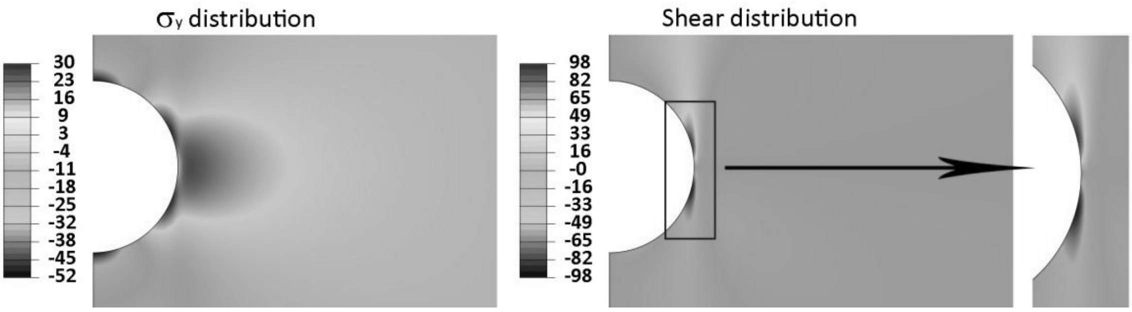

Figure 8. Distribution of σ_y and τ close to the hole of the CFRP lamella [MPa].

Comparing Figure 8 and Figure 3, it can be seen that the highest value of σ_x, σ_y and τ are found at different locations. The absolute values of σ_y and τ are much lower than σ_x. Three classical strength criterions Azzi-Tsai-Hill, Tsai-Hill and Tsai-Wu strength theory (Jones 1998) are chosen to evaluate the CFRP resistance. According to these three strength criterions, the failure starting location of this CFRP lamella is determined by FEM analysis and shown in Figure 9. The failure occurs where the value is higher than 1.0 in ABAQUS simulation.

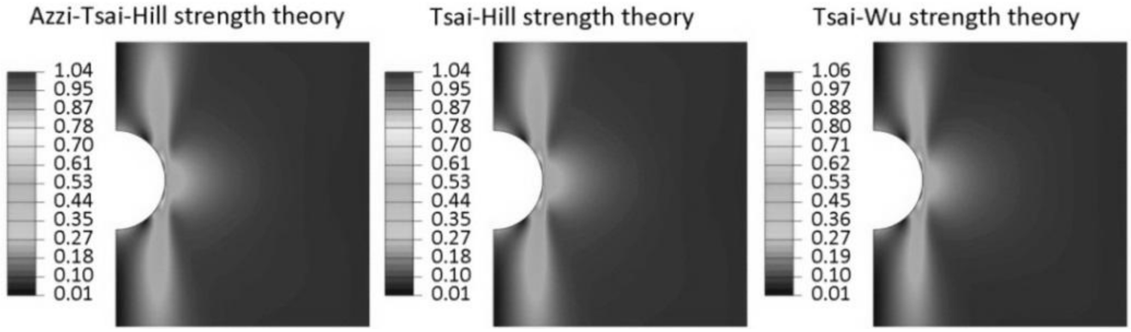

Figure 9. Failure starting location of the CFRP lamella determined by strength criterions.

As can be seen from Figure 9, the failure does not start at the intersection point of the *y*-axis with the edge of the hole. It starts close to the shear concentration points. Failure starts with a tension of 160 MPa. The same result can be observed during the experiment (see Figure 10).

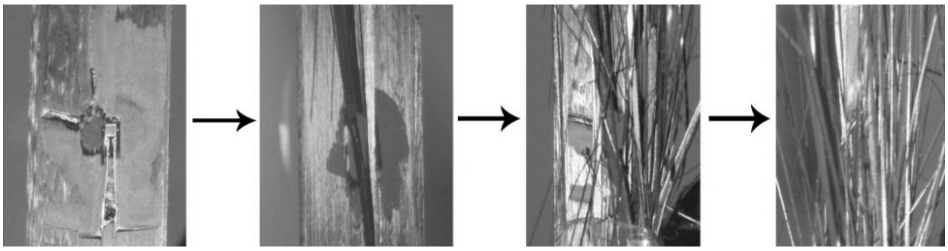

Figure 10. Failure starting location and failure process during the experiment.

The failure starts with a longitudinal crack of the matrix. The location of the crack is similar to that one predicted by the FEM analysis. The failure starting load in the experiment is approximately 160 MPa. With the increase of tension load, the crack rapidly penetrates the specimen in longitudinal direction. However, the load bearing capacity of the specimen is hardly reduced. When the load reached approximately 2150 MPa, the fibres in one side of the hole suddenly brake. Just after that the fibres on the other side also crack so that the whole specimen is destroyed.

In order to clarify the failure type, Hashin criterion is applied into the corresponding FEM model in ABAQUS. Hashin criterion classifies the failure types of CFRP lamella into 4 categories: fibre tensile failure, fibre compressive failure, matrix tensile failure and matrix compressive failure (Hashin 1980). When the tension load reaches 160 MPa, the FEM result from Hashin criterion is what is shown in Figure 9. Failure starts with a matrix tensile crack.

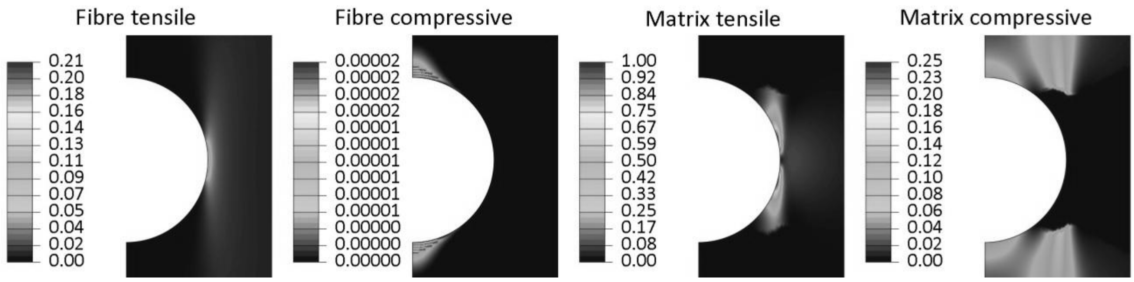

Figure 11. FEM result of the four failure modes based on Hashin criterion.

Figure 11 shows that only the matrix tensile failure happens while the other failure modes are small. The location is generally the same as predicted from the other three criterions. Hence, it is clear that the CFRP lamella starts with matrix tensile failure which is also proven by the experiment observation.

The experiment shows, that the tension load is mainly taken by the fibres. The simulation of the failure process based on fibre tensile failure mode (Hashin criterion) is shown in Figure 12.

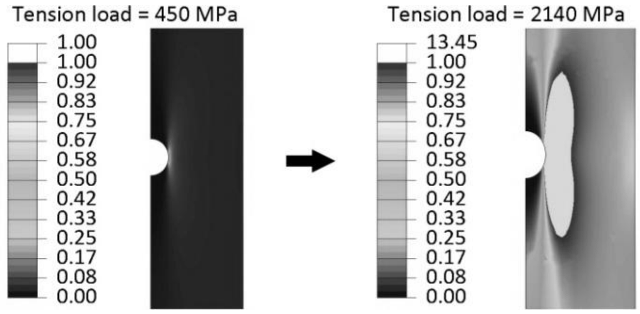

Figure 12. CFRP fibre failure process based on Hashin criterion

It can be seen in Figure 12 that the fibre tensile failure begins at a tension load of 450 MPa. When the tension load increases up to 2140 MPa the fibre tensile failure zone almost penetrates all the cross section. This introduces the failure of the lamella. The failure stress coincides well with the experiment result.

4 CONCLUSION

From the research for this paper, two main conclusions can be gained.

1) The stress concentration level in CFRP lamellas is much higher than that in steel lamellas. The shapes of their σ_x distribution curves are similar but that one from CFRP lamellas declines faster. These phenomena can be attributed to the strong orthotropic property of CFRP. A semi-empirical equation was suggested to calculate the *SCF* for the CFRP lamella with finite width.

2) The failure of CFRP lamella does not start at the intersection point of the *y*-axis with the edge of the hole but close to the shear concentration region. The failure process of CFRP lamellas begins with a tensile failure of polymer matrix and ends with a wide range of tensile failure of carbon fibre.

REFERENCES

Gibson, RF. 2007. *Principles of Composite Material Mechanics, 2th Edition.* Boca Raton: CRC Press, Inc.

Giulio R. 2001. Analytical and experimental behaviour of laminated panels with rectangular opening under biaxial tension, compression and shear loads. *Journal of Composite Materials*, 35: 639-663.

Hashin, Z. 1980. Failure Criteria for Unidirectional Fiber Composites. *Journal of Applied Mechanics*, 47: 329–334.

Jones MR. 1998. *Mechanics Of Composite Materials 2th Edition.* Boca Raton: CRC Press, Inc.

Lekhnitski SG. 1981. *Theory of elasticity of an anisotropic body*. San Francisco: Mir Publisher, Inc.

Schlaich, M. et al. 2012. CFK-Zugelemente und ihre Verankeungen. Bautechnik, 89: 841-850.

Timoshenko, SP and Gere, JM. 1961. *Theory of Elastic Stability.* New York: Dover Publications, Inc.

Wu, HC and Mu B. On stress concentrations for isotropic/orthotropic plates and cylinders with a circular hole. *Composite Part B*, 34:127-134.